ISSN 1674-1056
http://cpb.iphy.ac.cn
http://iopscience.iop.org/cpb
中国物理 B
Chinese Physics
中国物理 Chinese Physics B

Ultraviolet photodetectors based on wide bandgap oxide semiconductor films

Changqi Zhou(周长祺), Qiu Ai(艾秋), Xing Chen(陈星), Xiaohong Gao(高晓红), Kewei Liu(刘可为), Dezhen Shen(申德振)

Citation: Chin. Phys. B . 2019, 28(4): 048503. **doi:** 10.1088/1674-1056/28/4/048503
Journal homepage: http://cpb.iphy.ac.cn; http://iopscience.iop.org/cpb

What follows is a list of articles you may be interested in

Effect of temperature on photoresponse properties of solar-blind Schottky barrier diode photodetector based on single crystal Ga_2O_3

Chao Yang(杨超), Hongwei Liang(梁红伟), Zhenzhong Zhang(张振中), Xiaochuan Xia(夏晓川), Heqiu Zhang(张贺秋), Rensheng Shen(申人升), Yingmin Luo(骆英民), Guotong Du(杜国同)

Chin. Phys. B . 2019, 28(4): 048502. **doi:** 10.1088/1674-1056/28/4/048502

Realizing photomultiplication-type organic photodetectors based on C_{60}-doped bulk heterojunction structure at low bias

Wei Gong(龚伟), Tao An(安涛), Xinying Liu(刘欣颖), Gang Lu(卢刚)

Chin. Phys. B . 2019, 28(3): 038501. **doi:** 10.1088/1674-1056/28/3/038501

Recent advances in Ga-based solar-blind photodetectors

Ming-sheng Xu(徐明升), Lei Ge(葛磊), Ming-ming Han(韩明明), Jing Huang(黄静), Hua-yong Xu(徐化勇), Zai-xing Yang(杨再兴)

Chin. Phys. B . 2019, 28(2): 028502. **doi:** 10.1088/1674-1056/28/2/028502

Transition of photoconductive and photovoltaic operation modes in amorphous Ga_2O_3-based solar-blind detectors tuned by oxygen vacancies

Yan-Fang Zhang(张彦芳), Xuan-Hu Chen(陈选虎), Yang Xu(徐阳), Fang-Fang Ren(任芳芳), Shu-Lin Gu(顾书林), Rong Zhang(张荣), You-Dou Zheng(郑有炓), Jian-Dong Ye(叶建东)

Chin. Phys. B . 2019, 28(2): 028501. **doi:** 10.1088/1674-1056/28/2/028501

Metal halide perovskite photodetectors: Material featuresand device engineering

Ye Wang(王烨), Meng-Lei Gao(高孟磊), Jin-Liang Wu(吴金良), Xing-Wang Zhang(张兴旺)

Chin. Phys. B . 2019, 28(1): 018502. **doi:** 10.1088/1674-1056/28/1/018502

TOPICAL REVIEW — Photodetector: materials, physics, and applications

Ultraviolet photodetectors based on wide bandgap oxide semiconductor films*

Changqi Zhou(周长祺)[1,2,†], Qiu Ai(艾秋)[1,2,†], Xing Chen(陈星)[1,‡], Xiaohong Gao(高晓红)[1,2], Kewei Liu(刘可为)[1,§], and Dezhen Shen(申德振)[1]

[1] *State Key Laboratory of Luminescence and Applications, Changchun Institute of Optics, Fine Mechanics and Physics, Chinese Academy of Sciences, Changchun* 130033, *China*

[2] *University of Chinese Academy of Sciences, Beijing* 100049, *China*

(Received 1 January 2019; revised manuscript received 24 February 2019; published online 19 March 2019)

Ultraviolet (UV) photodetectors have attracted more and more attention due to their great potential applications in missile tracking, flame detecting, pollution monitoring, ozone layer monitoring, and so on. Owing to the special characteristics of large bandgap, solution processable, low cost, environmentally friendly, *etc*., wide bandgap oxide semiconductor materials, such as ZnO, ZnMgO, Ga_2O_3, TiO_2, and NiO, have gradually become a series of star materials in the field of semiconductor UV detection. In this paper, a review is presented on the development of UV photodetectors based on wide bandgap oxide semiconductor films.

Keywords: photodetector, ultraviolet, oxide semiconductor film

PACS: 85.60.Gz, 61.80.Ba, 61.82.Fk **DOI:** 10.1088/1674-1056/28/4/048503

1. Introduction

In recent years, ultraviolet (UV) photodetectors have gained extensive attention of researchers worldwide owing to their potential applications in solar UV radiation detection, missile tracking, flame detection, ozone monitoring, environmental monitoring, *etc*.[1–4] Although GaN and SiC based UV photodetectors possess mature manufacturing technologies and thus have already been commercialized,[5–7] it is still tough to further reduce the cost and improve the performance for wide applications. Wide bandgap oxide semiconductors, including ZnO, ZnMgO, Ga_2O_3, TiO_2, NiO, and so on, are the focus of current research efforts since they have special physical and chemistry properties, such as stability, environmental friendliness, and enrichment of raw materials.[8–12] Till now, the UV photodetectors based on wide bandgap oxide semiconductors with various device structures have been demonstrated, including p–n junction, Schottky junction, metal–semiconductor–metal (MSM) structure, and heterojunction. Several review articles have been published on ZnO-based UV photodetectors and metal–oxide nanostructure photodetectors.[13–17] Liu *et al.* summarized the history and the development of ZnO-based photodetectors.[13] Hou *et al.*[14] and Yang *et al.*[15] focused on the performances of ZnO-based UV photodetectors and the relevant physics. Zhai *et al.*[16] and Tian *et al.*[17] discussed several kinds of important metal–oxide nanostructures (such as ZnO, SnO_2, Ga_2O_3, Cu_2O, Fe_2O_3, In_2O_3, CdO, CeO_2, Nb_2O_5, and WO_3) and their corresponding photodetector applications.

In this review, we will first discuss the technical development of ZnO-based UV photodetectors, followed by recent advances of UV photodetectors based on Ga_2O_3, TiO_2, and NiO. Finally, a brief summary, challenge, and prospect will be given.

2. ZnO-based film photodetectors

ZnO is one of the most prominent members of the family of wide bandgap oxide semiconductor due to its unique physical and chemical properties.[18–20] It has strong radiation hardness, high chemical stability, low cost, and a large bandgap of 3.37 eV at room temperature.[21–23] Furthermore, by alloying ZnO with MgO, the bandgap of $Zn_xMg_{1-x}O$ can be adjusted from 3.37 eV to 7.8 eV,[24,25] which is essential to fabricate UV photodetectors with different cut-off wavelengths. These properties are crucial for practical optoelectronic devices used in missile warning system, flame detection, and inter-satellite communications.[26–28] In addition, ZnO and its alloy ZnMgO materials are environment-friendly and rich in natural resources. Therefore, ZnO-based material is one of the best

*Project supported by the National Natural Science Foundation of China (Grant Nos. 61475153 and 61605200), the Jilin Province Young and Middle-aged Science and Technology Innovation Leaders and Team Project, China (Grant No. 20180519023JH), the 100 Talents Program of the Chinese Academy of Sciences, and the Science Fund for Excellent Young Scholars of Jilin Province, China (Grant No. 20180520173JH).

†These authors contributed equally to this work.

‡Corresponding author. E-mail: chenxing@ciomp.ac.cn

§Corresponding author. E-mail: liukw@ciomp.ac.cn

© 2019 Chinese Physical Society and IOP Publishing Ltd

candidate materials for preparing UV photodetectors.[29–33]

After years of development, UV photodetectors based on ZnO and ZnMgO films have made great process, which has been discussed in the previous reviews.[13–15] Notably, to improve the performance of ZnO-based UV photodetectors, various methods have been selected, such as surface treatment, surface plasmonic effect, mixed-phase material, and so on. In this section, we will describe several ways to improve the performance of ZnO-based photodetectors.

2.1. Surface treatment

According to previous reports, ZnO exhibited a strong adsorption/desorption behavior of oxygen on the surface, which had a very big influence on the properties of ZnO-based UV photodetectors.[34,35] For example, these adsorption/desorption processes of oxygen on the surface of ZnO could lead to a long rise/decay time of bare ZnO-based UV photodetectors.[36,37] In order to improve the performance of ZnO-based UV detectors, scientists have studied many methods, such as oxygen plasma treatment,[38–41] surface passivation,[35,39,42] solution treatment,[43–45] and so on. In 2003, Coppa *et al.*[38] cleaned the ZnO (000-1) surface by O_2/He plasma, which could significantly improve the rectifying characteristics of Au/ZnO junction. Liu *et al.*[46] treated the ultrathin (20-nm-thick) ZnO epitaxial films with oxygen-radical-rich inductively coupled plasma to improve the performance of detectors (the decay time was reduced to below 50 μs and the on/off ratio was increased over 1000). In 2007, Angadi *et al.*[47] studied the effect of oxygen plasma treatment on the performance of Au–ZnO–In photodetectors, and a good Schottky junction detector with high UV responsivity (160 A/W at 254 nm) could be obtained after the treatment. In 2012, Reyes *et al.*[48] prepared a ZnO UV photodetector based on a thin film transistor (TFT), and the persistent photoconductivity of the device was suppressed through oxygen plasma treatment. Figure 1(a) shows the turn-off times of the untreated device, and the device with oxygen plasma treatment. The surface-treated device yields a reduced turn-off time of 10 ms as compared to 26 ms turn-off time of the untreated device. Figures 1(b) and 1(c) show O_{1s} peaks in x-ray photoelectron spectroscopy (XPS) spectra of the untreated ZnO channel and the O_2 plasma treated ZnO channel, respectively. The peak appearing at the lower binding energy 530.68 eV (O_I) is due to the O^{2-} ions presenting in the stoichiometric ZnO; on the other hand, the peak at the higher binding energy $\sim$ 532.38 eV (O_{II}) could be attributed to O^{2-} ions in oxygen deficient ZnO. The ratio of the peak area due to the oxygen deficient ZnO over the total area of the two peaks (O_{II}/O_{tot}) indicates the relative quantity of this oxygen-related defect. According to the results of XPS measurements, the improvement of recovery time for the photodetector is achieved through the suppression of persistent photoconductivity using oxygen plasma treatment to reduce the oxygen vacancies.

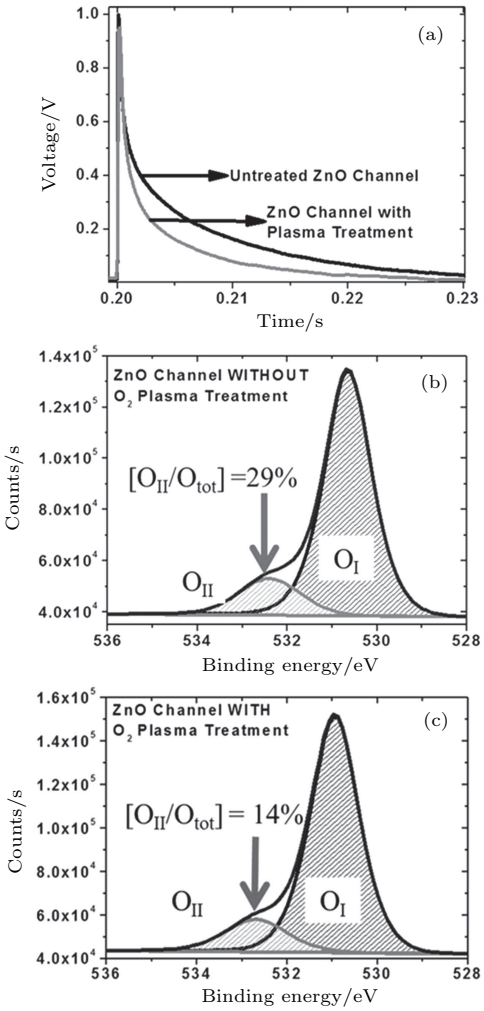


Fig. 1. (a) Recovery times of the ZnO-TFT UV photodetector with and without channel surface treatment; XPS spectra of (b) untreated ZnO channel, and (c) oxygen plasma-treated ZnO channel.[48]

In addition to oxygen plasma, the surface treatment by solution is also a common method to improve the performance of ZnO-based photodetectors, and this method has been widely used in the devices based on ZnO micro/nanostructures.[49–52] Recently, scientists have introduced this method into ZnO thin film detectors. In 2017, Zhu *et al.*[36] investigated the effect of H_2O_2 solution treatment on the properties of the ZnMgO thin film and its UV photodetectors. After the treatment by H_2O_2 solution, the dark current of ZnMgO UV photodetectors decreased by more than one order of magnitude. Moreover, the response time of the device could be significantly reduced both in vacuum and an oxygen atmosphere by H_2O_2 solution treatment due to the reduction in the oxygen vacancy defects in ZnMgO. However, the responsivity would also be obviously decreased using this method.

More recently, Chen *et al.*[37] demonstrated a performance enhancement of ZnMgO photodetectors through HF solution treatment. As shown in Fig. 2, after the treatment

with HF solution, the dark current decreases from 0.7 pA to 0.4 pA, and the peak responsivity of the device increases from 145 A/W to 326 A/W at 10 V. Additionally, the 90%–10% decay time of the device is decreased by more than one order of magnitude (from 4.6 ms to 0.34 ms). Large amounts of Zn–F or Mg–F on the ZnMgO surface should be responsible for the performance enhancement after HF treatment. The F-modified surface of ZnMgO film could adsorb more O_2 molecules and induce more oxygen-related hole-trap states due to the strong O_2 adsorption ability, resulting in low dark current and larger responsivity. Moreover, after turning off the UV light, the oxygen molecules are reabsorbed on the surface of ZnMgO and capture the free electrons more quickly, thus the smaller t-decay is achieved. This result indicates that the chemical treatment with HF solution should be a useful and effective method for improving the performance of ZnMgO UV photodetectors.

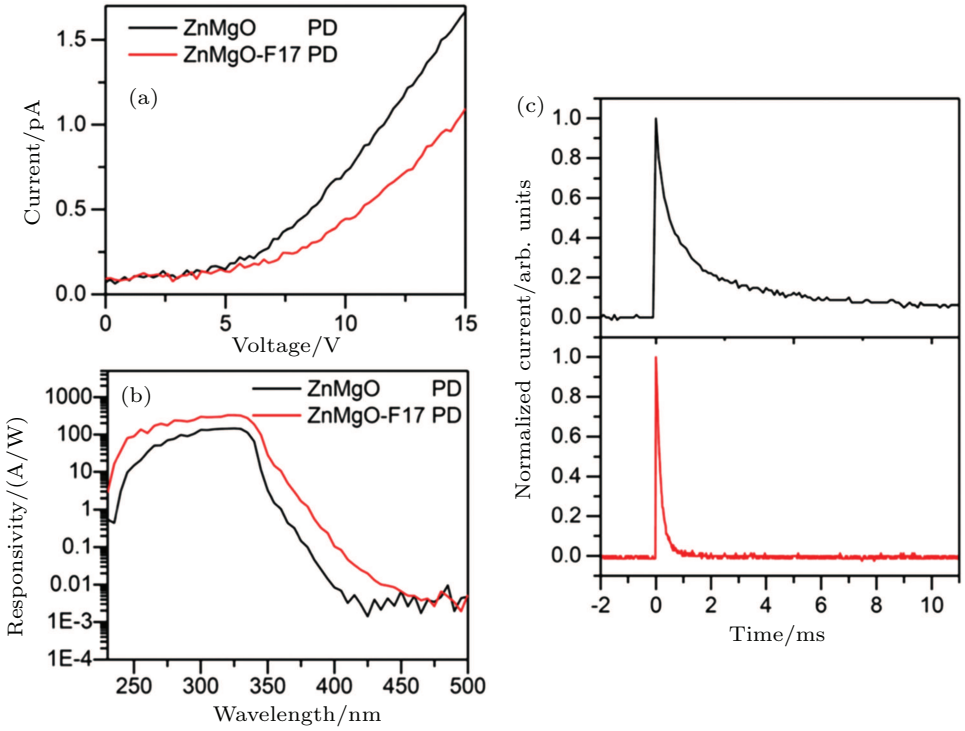


Fig. 2. (a) *I–V* characteristics of devices in the dark. (b) Spectral responses of the devices under a bias of 10 V. (c) Decay edge of the current response at a bias of 10 V.[37]

2.2. Surface plasmonic effect

Surface plasmons (SPs) are collective oscillations of free electrons between metal and dielectric (semiconductor) materials, which have also been employed to enhance the performance of photodetectors.[53–64]

In 2014, Tian *et al.*[56] reported that Pt nanoparticles could be used to enhance the performance of the UV photodetectors, where surface plasma resonance occurs. Figure 3 shows the response spectra of the ZnO MSM structure UV photodetectors before and after sputtering of Pt nanoparticles. It can be seen that the responsivity of the device is enhanced from 0.836 A/W to 1.306 A/W by sputtering Pt nanoparticles on the surface of the device. After that, Pei *et al.*[57] demonstrated that the maximum responsivity enhancement ratio of ZnO MSM sandwich UV photodetectors could range from 14 to 45 times by adjusting the embedded depth of the Pt nanoparticles. In 2014, Li *et al.*[59] fabricated high-performance ZnO-based MSM UV photodetectors decorated with Ag nanoparticles by a chemical method positioned. After the introduction of the Ag nanoparticles, the responsivity of the device was enhanced from 472 mA/W to 51.3 A/W, but the dark current also increased. After that, their group reported the responsivity enhancement (from 472 mA/W to 10.522 A/W) of Ag nanoparticles-embedded ZnO film UV photodetector without the apparent increase of dark current.[60] In 2016, Sun *et al.*[61] fabricated ZnO semiconductor films with periodic 3D nanocave patterns, and the Au nanoparticles were subsequently introduced into the ZnO film, which could boost the UV responsivity and extend the photodetection to the visible light region.

Compared to the traditional dipole plasmon resonance, high-order plasmon modes are often excited in the shorter-wavelength range, which is expected to be used to improve the UV-detection performance. Moreover, a highly wavelength-selective UV response enhancement for ZnO photodetectors could be achieved due to the narrow-band quadrupole resonance. In 2017, Ag nanoparticles-decorated ZnO photodetectors were proposed by Wang *et al.*,[62] and the device exhibited an obvious increase in peak responsivity at around 380 nm, which could be attributed to the narrow-band quadrupole plas-

mon resonance of Ag nanoparticles in the UV range. Figure 4 shows the properties of UV photodetector based on ZnO thin film with and without Ag nanoparticles. The dark current of the device is decreased by the introduction of Ag nanoparticles. More interestingly, after covering with Ag nanoparticles, the intensity of the response peak increases obviously from 2.16 A/W to 2.86 A/W, while the responsivity at the other wavelengths decreases a lot, resulting in the full width at half-maximum of response peak as narrow as $\sim$ 10 nm. Moreover, the response speeds of the ZnO UV photodetectors with and without Ag nanoparticles have no significant change. By coating Ag nanoparticles on the ZnO surface, a localized Schottky junction can be formed at the interface, and the wavelength of the ultraviolet light is coupled to the resonant frequency of the Ag nanoparticles. Thus, the performance of device could be enhanced obviously. This work would open a way to harness the high order plasmon modes in the field of UV optoelectronic devices.

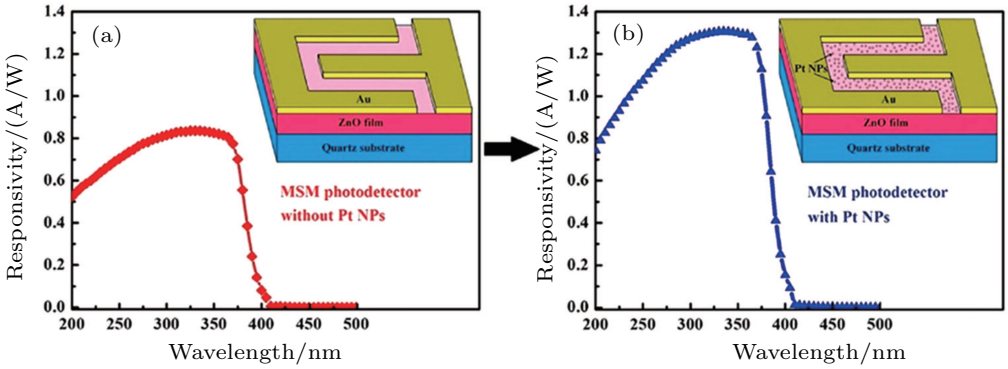


Fig. 3. Response spectra of the ZnO MSM structure UV photodetectors before and after sputtering of Pt nanoparticles. The inset shows the schematic illustration of the device.[56]

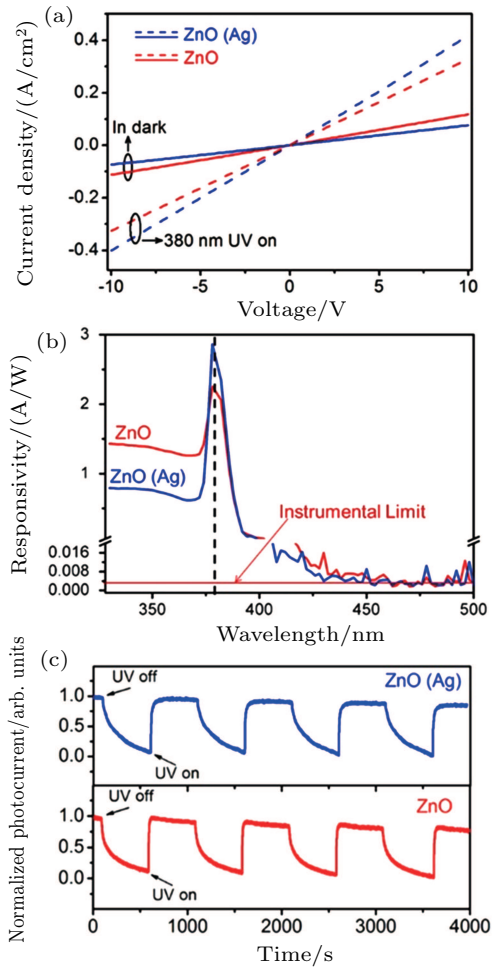


Fig. 4. (a) *J*–*V* characteristics in dark condition and (b) response spectra of the ZnO UV photodetectors with and without Ag nanoparticles under 15-V bias. (c) Time-dependent photocurrent with periodic switching of UV illumination (380 nm) measured at 30-V bias.[62]

In brief, the performance of ZnO-based photodetector has been significantly improved by introducing metal plasmon resonance, and these results could provide a promising way to develop high-performance UV photodetectors.

2.3. Mixed-phase material

As is well known, ZnO is stabilized in the hexagonal wurtzite structure, while MgO is stabilized in the cubic rock salt structure. Therefore, the crystal structure of ZnMgO alloy would change from wurtzite structure to cubic structure as the Mg content increases. And ZnMgO with both hexagonal and cubic phases is commonly obtained in the previous reports, which could be called mixed-phase ZnMgO. It could be found that the photodetectors fabricated on mixed-phase ZnMgO exhibit a relatively higher responsivity than that of the single-phase devices.[31,65,66] Thus, preparing mixed-phase material may be a viable method to improve the performance of ZnMgO UV photodetectors. However, the mixed-phase ZnMgO usually has two absorption edges: one is shorter than 280 nm and the other is longer than 300 nm, indicating that they are not suitable for solar-blind detection without external filters.[18,67–70]

In 2014, a mixed-phase $Zn_{0.38}Mg_{0.62}O$ film with a single absorption edge has been firstly deposited on a-face sapphire using plasma-assisted molecular beam epitaxy by Fan *et al.*[71] Furthermore, a mixed-phase ZnMgO UV photodetector with excellent comprehensive performance has been fabricated. The device showed only one response peak at 260 nm with the responsivity of 1.664 A/W which is differ-

ent from other mixed-phase ZnMgO photodetectors containing two photoresponse bands. In addition, the dark current of the device was only 0.25 pA at 5 V, which was much lower than that of the reported mixed-phase ZnMgO photodetectors. After that, Fan *et al.* further studied the carrier transport process of mixed-phase ZnMgO photodetector at different conditions, such as thermal equilibrium, dark, and UV illumination, as shown in Fig. 5,[72] and tried to find out the reason for the excellent optoelectrical characteristic for the devices. They found that large amounts of heterojunctions between wurtzite-phase ZnMgO (w-ZnMgO) and cubic-phase ZnMgO (c-ZnMgO) in the mixed-phase ZnMgO film should be responsible for the ultra-low dark current; meanwhile, the high-resistance of c-ZnMgO film also plays an important role in producing low dark current. Under the radiation of UV light, photogenerated holes were trapped at the interfaces between w-ZnMgO and c-ZnMgO, prolonging their lifetimes. At the same time, the barrier height at grain boundary can be reduced, enhancing the electron conductance and reducing the electron-transit time. The longer lifetime could increase the internal gain and then increase the responsivity. After this study, some scientists began to focus on the mixed-phase ZnMgO UV photodetector. Han *et al.*[73–75] fabricated MSM structure UV detectors based on mixed-phase ZnMgO thin films by pulsed laser deposition (PLD) method, and the effect of the substrate surface atom constitution and the migration characteristics of reactive atoms on crystal structure of the ZnMgO thin films have been investigated.

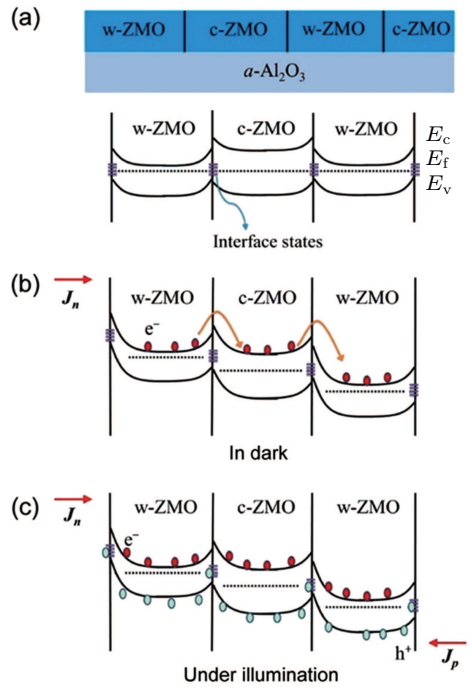


Fig. 5. Energy band diagram and carrier transport process of mixed-phase ZnMgO photodetector at different conditions: (a) at thermal equilibrium, (b) under bias in dark, and (c) under bias with UV illumination.[72]

In addition, several other methods have been used to improve the performance of ZnO-based UV photodetectors.[76–85] For example, Tian *et al.* and Wang *et al.*[82,83] developed the high performance ZnO nanosheet field-effect transistor by using ferroelectric to get the very low dark current. The device reveals an improved optical response and detectivity up to 3.8×10^5 A/W and 4.4×10^{15} Jones (unit Jones: cm·Hz$^{1/2}$·W^{-1}), and the photocurrent gain is 1.24×10^6. At the same time, Wang *et al.*[84] fabricated a high performance ZnO nanosheet photodetector driven by the charge transfer induced local field. The photodetector exhibits ultralow dark current (10^{-12} A), ultra-high specific detectivity (up to $\sim 10^{14}$ Jones), and fast rising (300 ms) and decaying times (310 ms).

Due to space limitations, we only summarize the above methods used to improve the performance of ZnO UV photodetectors (PDs). Although ZnO-based UV photodetectors have made great progress in recent years, there are still some problems remaining to be solved. For example, the lack of stable and reproducible p-type ZnO-based materials, the low responsivity of MgZnO solar-blind PDs, the slow response speed, and so on. Therefore, more research should be performed to address these challenges.

3. Ga_2O_3-based film photodetectors

Solar-blind UV photodetectors can accurately response to a very weak signal even under sun or room illumination. Monoclinic Ga_2O_3 (β-Ga_2O_3), with an intrinsic bandgap E_g of ~ 4.9 eV and accordingly a corresponding wavelength of ~ 260 nm,[86–91] is naturally suitable for solar-blind UV detection. Consequently, Ga_2O_3 has attracted much attention recently, and its characteristics of solar-blind UV detection have been demonstrated in various device structures, including MSM structure, Schottky junction, and heterojunction structure.[92–103]

3.1. MSM structure

MSM structure photodetectors have the advantages of simple structure, easy preparation, *etc*. In 2007, Kokubun *et al.*[104] grew β-Ga_2O_3 MSM photodetectors using sol–gel method, and the maximum responsivity of the device was only 8×10^{-5} A/W. In 2014, Guo *et al.*[105] deposited β-Ga_2O_3 epitaxial thin films using laser molecular beam epitaxy (L-MBE) technique, and *in situ* annealing on the film under oxygen atmosphere could lead to the transition of the Au/Ti electrode/β-Ga_2O_3 thin film from ohmic to Schottky contact due to the reduction of the oxygen vacancy. Figure 6 shows the time-dependent photoresponse of the β-Ga_2O_3 thin films prototype photodetector to 254-nm illumination. The dark current, rise time, and decay time for the Schottky type photodetectors are only 0.3 nA, 0.62 s, and 0.83 s, respectively. Compared with the Ohmic-type photodetector, the Schottky-type photodetector shows lower dark current, higher photocurrent/dark current

ratio, and shorter switching time, which benefit from Schottky barrier controlling electron transport and the significant reduction in the quantity of photogenerated carriers trapped by oxygen vacancy.

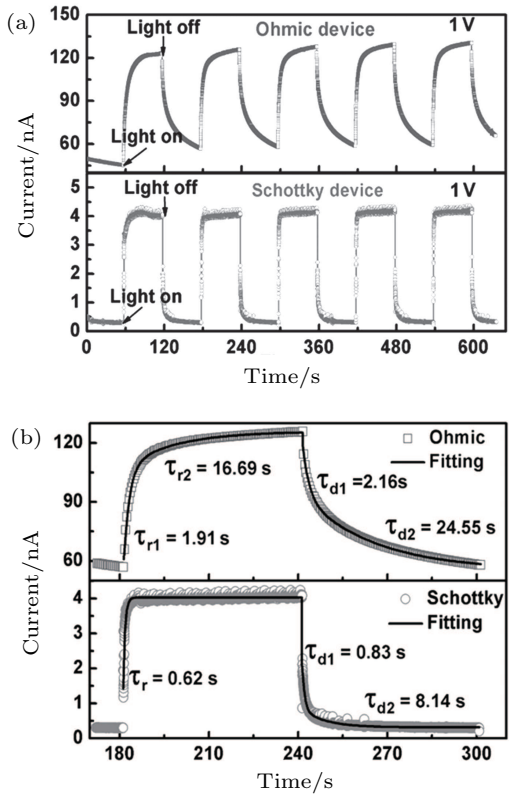


Fig. 6. Time-dependent photoresponse of the β-Ga_2O_3 thin films prototype photodetector to 254-nm illumination: (a) the ohmic-type device and the Schottky-type device; (b) enlarged view of the rise/decay edges and the corresponding exponential fitting for the ohmic-type device and Schottky type devices, respectively.[105]

In 2015, Hu *et al.*[106] deposited β-Ga_2O_3 film using metalorganic chemical vapor deposition (MOCVD) technique, and the photodetectors with interdigitated electrodes have been designed and fabricated on this film. The device exhibited a responsivity of 17 A/W, a UV-to-visible rejection ratio of 8.5 $\times 10^6$, and a quantum efficiency of around 8228% at 20-V bias. In 2017, Alema *et al.*[107] reported the fabrication and characterization of solar-blind photodetectors based on undoped β-Ga_2O_3 and Zn-doped β-Ga_2O_3 (ZnGaO) epitaxial films with a cutoff wavelength of 260 nm. The ZnGaO detector showed a peak responsivity of 210 A/W at 232 nm, which is much higher than that for β-Ga_2O_3 device (46 A/W). In 2018, Zhang *et al.*[108] grew high quality β-Ga_2O_3 film by using N_2O as reaction gas for the fabrication of high performance solar-blind photodetector. This device exhibited a high responsivity of 26.1 A/W. And the rise and decay times were around 0.48 s and 0.18 s at 10 V, respectively. The excellent performance can be attributed to the reduction of scattering or/and trapped center of photo-generated carriers formed in the film grown with N_2O.

3.2. Schottky junction

Considering the potential applications in secure communication and space detection, the quick response speed and the self-powered ability for a solar-blind photodetector are strongly desirable. The vertical Schottky photodiode should satisfy this requirement. In 2016, an Au/β-Ga_2O_3 nanowires array film vertical Schottky photodiode was successfully fabricated by a simple thermal partial oxidation process.[109] The device had a four-layer structure, namely, Au/β-Ga_2O_3 nanowires array/β-Ga_2O_3 film/Ga. This Schottky type photodetector showed an obvious solar-blind response without any power supply, and 90%–10% decay time is only 64 μs.

3.3. Heterojunction structure

Weng *et al.*[110] reported the fabrication of a β-Ga_2O_3/GaN dual-band photodetector. The dark current of the device was only 3.58×10^{-11} A at 5-V applied bias and the near-UV to visible contrast ratio was 850 at 10-V bias. In 2016, Guo *et al.*[111] fabricated β-Ga_2O_3 thin films on p-type silicon (100) substrates by laser molecular beam epitaxy, and the heterojunctions were then formed as a deep UV solar-blind photodetector. The responsivity of the device reached 370 A/W at 3 V reverse bias at 254 nm, and the corresponding external quantum efficiency was over 1.8×10^5%, which can be attributed to the carrier multiplication. In addition, the rise time and fall time were 1.79 s and 0.27 s, respectively. In the same year, Qu *et al.*[112] grew β-Ga_2O_3 films on n-type 4H-SiC substrates using laser molecular beam epitaxy technique. By replacing Au/Ti with single-layer graphene as the top electrode, the responsivity increased from 7.14×10^{-4} A/W to 0.18 A/W, and the rise time decreased from 2.14 s to 0.65 s. These results suggested that the graphene transparent electrodes could not only allow the majority of the incident light to reach the contact area, but also offer an easy carrier transport channel when the electron-holes were separated.

In addition, metastable α-phase Ga_2O_3 is an emerging material for developing solar-blind photodetectors. In 2017, Chen *et al.*[113] realized single crystalline α-Ga_2O_3 epilayers on nonpolar ZnO substrates and a high performance Au/α-Ga_2O_3/ZnO isotype heterostructure-based Schottky barrier avalanche diode was demonstrated. The device displayed a rise time of 238 μs and a decay time of 3040 μs. In addition, the responsivity at 254 nm could reach 1.10×10^4 A/W at −40-V bias.

Although great progress has been made in Ga_2O_3 photodetectors, the responsivity remains relatively low. Besides, p-type doping of Ga_2O_3 is still a bottleneck problem which severely limits its application in the optoelectronic system. Furthermore, the severe persistent photoconductivity effect should be addressed in the future.

4. TiO_2-based film photodetectors

The wide bandgap of TiO_2 (3.2 eV for anatase and 3.0 eV for rutile structure) makes it very suitable for UV detection applications.[114] Till now, TiO_2-based UV photodetectors, including MSM structure, Schottky structure, and heterojunction structure, have been demonstrated and investigated.

4.1. MSM structure

Up to now, most of the reported TiO_2 UV photodetectors are based on MSM structure. In 2007, anatase TiO_2 MSM photodetectors were fabricated by sol–gel method on Si substrate.[115] At 5-V bias, the dark current and the responsivity at 260 nm were around 1.9 nA and 199 A/W, respectively. However, the device showed a slow response with a rise time of 6 s and a decay time of 15 s. In 2009, Kong *et al.*[116] fabricated TiO_2 MSM photodetectors with Ni electrode. At 5-V bias, the dark current of the detector was only 1.83 nA, and the responsivity at 260 nm can be as high as 889.6 A/W. This large responsivity could be explained by the great internal gain associated with the hole trapping at interface. In 2011, Shih *et al.*[117] fabricated oxygen plasma modified TiO_2 MSM photodetectors using radio frequency (RF) magnetron sputtering. The spectral responsivities of the fabricated TiO_2 MSM photodetectors with different oxygen plasma treatment times were investigated. It was found that the cutoff wavelength is close to 387 nm. With a 360-nm illumination and 5-V applied bias, it was found that the maximum responsivities of the fabricated TiO_2 photodetectors with oxygen plasma treatment of, 1 min, 2 min, and 3 min were 36 A/W, 144 A/W, 153 A/W, and 53 A/W, respectively.

4.2. Schottky structure

There are very few reports about TiO_2-based Schottky-type UV PDs. Akbari *et al.*[118] fabricated monolayer TiO_2 film based photodetector via atomic layer deposition. The device displayed a responsivity of 0.352 A/W at 1-V bias with short rise (30 μs) and fall time (63 μs). The I_{on}/I_{off} ratio was about 220 with an excellent stability. Patel *et al.*[119] reported Cu/TiO_2/FTO Schottky type photodetectors fabricated by direct current (DC) sputtering technique. At −1-V bias, the peak responsivity and detectivity were 0.897 A/W and 4.5×10^{12} Jones, respectively. In addition, the device showed a very quick response speed with a rise time of 1.12 ms and a fall time of 1.46 ms.

4.3. Heterojunction structure

Zhang *et al.*[120] prepared TiO_2 nanocrystalline films on $SrTiO_3$ (001) substrate to form a heterojunction active layer using a sol–gel method. At 10-V bias, the dark current of the detector was 0.2 nA and the responsivity was 46.1 A/W at 260 nm. The rise and fall times of the device were 3.5 ms and 1.4 s, respectively. Later, their group[121] fabricated a UV photodetector based on a TiO_2/NiO p–n heterojunction, which showed an overall improvement in performance (the dark current was 0.033 nA, the responsivity was 181.9 A/W at 280 nm, and the decay time was 598 ms) compared to their previous devices. The p–n heterojunction possessed the capacity of the majority carrier depletion due to its built-in electric field (E_{bi}) in dark, which has the potential to limit I_{dark} and the noise of devices. Sun *et al.*[122] fabricated a self-powered Fe-doped TiO_2/n-Si heterojunction UV-visible photodetectors via a facile solution process. The device displayed a responsivity of 46 mA/W (350 nm) and 60 mA/W (600 nm) with 0.5 mW/cm^2 light irradiation at zero bias. And the rise and decay times of the device were less than 10 ms and 15 ms, respectively. Liu *et al.*[123] deposited an ultrathin TiO_2 film on single crystal diamond surface through radio frequency magnetron sputtering method to form heterojunction PDs. The device showed two response peaks at around 225 nm (3 mA/W) and 290 nm (23.6 mA/W) stemming from the response of diamond and TiO_2, respectively, indicating a stretch of detection range of pure diamond or TiO_2 photodetector.

In summary, the research on TiO_2 as a material for UV photodetectors has just begun. At present, most of TiO_2 photodetectors were fabricated on nanomaterials. Therefore, more efforts should be concentrated on TiO_2 thin film photodetectors in the future.

5. NiO-based film photodetectors

Among various wide bandgap oxide semiconductors, nickel oxide (NiO) is a promising p-type semiconductor with a wide and direct energy band gap in the range of 3.2 eV–3.8 eV.[124–126] It has many advantages such as low cost, nontoxicity, earth abundance, transparency in the visible light, *etc*.[127–129] Therefore, NiO should be a good candidate for the fabrication of UV photodetectors.[130–133]

In 2009, Zhao *et al.*[134] used electron beam evaporation technique to grow Mg-doped NiO film on quartz substrate. The fabricated MSM photodetector displayed a peak responsivity of 0.147 mA/W at 320 nm and 5-V bias, and the dark current was about 70 nA. In 2017, Ahmed *et al.*[135] deposited NiO film on Si (100) substrate by using RF magnetron sputtering system, and the MSM photodetectors were then fabricated on this NiO film. Under 365- nm UV illumination at 5-V bias, the maximum responsivity was evaluated to be 4.5 A/W with a rise and fall time of 266 ms and 200 ms, respectively.

Owing to its p-type nature, NiO film has been mainly used to fabricate p–n heterojunction UV photodetectors with other n-type semiconductors, such as Si, ZnO, TiO_2, indium gallium zinc oxide (IGZO), and organic materials. In 2005, Choi *et al.*[136] evaporated NiO film on Si substrate to form p–n heterojunction, and the fabricated photodetectors showed

a responsivity at 290 nm of 0.15 A/W at 0 V. In 2014, Zhang *et al.*[137] demonstrated the p-NiO/n-Si heterojunction by the oxidation of Ni deposited on n-Si substrates, and the photodetector based on this heterojunction displayed a maximum responsivity of 0.815 A/W at −2-V bias. In 2015, Li *et al.*[138] fabricated n-IGZO/p-NiO photodetector on indium tin oxide (ITO) glass using magnetron sputtering technique. In Fig. 7(a), at −3-V bias, a peak responsivity of 0.016 A/W was observed at the wavelength of ∼ 370 nm with the full width at half maximum smaller than 30 nm. This high spectrum selectivity could be explained in terms of the "optically-filtering" function of the NiO layer. In addition, the performance of the photodetector was largely affected by the conductivity of the p-NiO thin film, which could be controlled by varying the oxygen partial pressure during the deposition of the p-NiO thin film, as shown in Fig. 7(b).

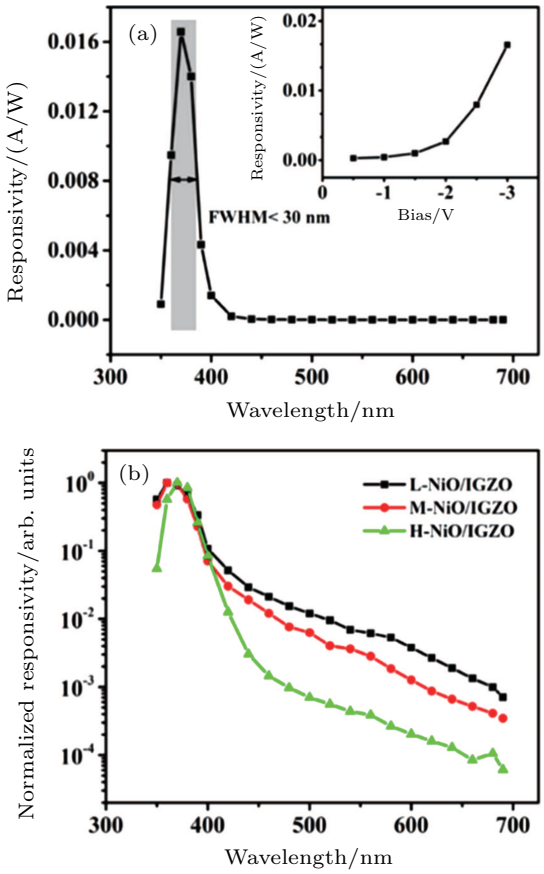


Fig. 7. (a) Spectral responsivity of the ITO/H-NiO (high conductivity NiO)/IGZO/ITO photodetector under the bias of −3 V. The inset shows the responsivity as a function of the reverse bias. (b) Normalized spectral responsivities of the ITO/L–NiO (low conductivity NiO)/IGZO/ITO, ITO/M–NiO (medium conductivity NiO)/IGZO/ITO, and ITO/H–NiO/IGZO/ITO photodetector structures at −3-V bias.[138]

Tsai *et al.*[139] fabricated p-NiO/n-ZnO by RF magnetron sputtering on glass substrate. The current–voltage curve of the heterojunction demonstrated obvious rectifying diode behavior in a dark environment. The lowest leakage current was 7.73×10^{-8} A/cm^2 for n-ZnO/p-NiO heterojunction diode. In 2017, Patel *et al.*[140] realized the high transparent self-powered heterojunction photodetector of the configuration of NiO/ZnO/ITO/polyethylene terephthalate (PET) by using the solid-state sputtering method. This high visible-range transparent (74.8%) photodetector was extremely sensitive to the tiny UV light density.

6. Conclusion and perspectives

This review has introduced ultraviolet photodetectors based on wide bandgap oxide semiconductor films, including ZnO, ZnMgO, Ga_2O_3, TiO_2, and NiO. The growth method of the materials, the classification of the photodetectors, and the development of performance of the devices have been reviewed and summarized. Recent progresses and challenges in this field are systematically discussed. Systematic comparison of photodetector performances based on these devices has been summarized in Table 1. It is clear that these devices will play a significant role in environmental monitoring, medical analysis, defense technology, and fire protection due to their special characteristics of large bandgap, solution processable, low cost, environmentally friendly, *etc*. Although many important progresses have been achieved on wide bandgap oxide semiconductor films, there is still a lot of work to be done in the field of UV photodetectors based on wide band gap oxide semiconductors, such as p-type doping, the improvement of the materials' quality, the design of the device structure, and so on.

Table 1. Comparison of the photodetector performances for wide bandgap oxide photodetector.

Structure	Dark current/nA	Peak responsivity/(A/W)	Rise time/ms	Decay time/ms	Ref.
ZnO MSM	0.4	10	–	0.05	[46]
ZnO MSM	5.65×10^6	160	–	–	[47]
ZnO TFT	5×10^{-5}	–	–	10	[48]
ZnO MSM	10	1.306	–	–	[56]
ZnO MSM	–	7	–	–	[57]
ZnO MSM	100	51.3	–	–	[59]
ZnO MSM	60	10.522	–	–	[60]
ZnO MSM	1	–	24000	15000	[61]
ZnO MSM	–	2.86	15000	330000	[62]
ZnMgO MSM	1×10^{-3}	4	–	< 1000	[36]
ZnMgO MSM	4×10^{-4}	326	–	0.34	[37]

Table 1. (*Continued*).

Structure	Dark current/nA	Peak responsivity/(A/W)	Rise time/ms	Decay time/ms	Ref.
ZnMgO MSM	2.5×10^{-4}	1.664	–	1000	[71]
ZnMgO MSM	4×10^{-3}	32	–	37	[72]
ZnO TFT	–	3.8×10^{5}	280	440	[83]
ZnO TFT	3.5×10^{-3}	6.83×10^{3}	300	310	[84]
Ga_2O_3 MSM	–	8×10^{-5}	–	–	[104]
Ga_2O_3 MSM	0.31	–	620	830	[105]
Ga_2O_3 MSM	0.62	17	–	–	[106]
ZnGaO MSM	0.02	210	3200	1400	[107]
Ga_2O_3 MSM	34	26.1	480	180	[108]
Ga_2O_3 Schottky	0.01	2.9×10^{-3}	0.001	0.06	[109]
Ga_2O_3/GaN	0.0358	~ 2	–	–	[110]
Ga_2O_3/Si	850	370	1790	270	[111]
Ga_2O_3/SiC	0.509	0.18	650	1730	[112]
Ga_2O_3/ZnO	1×10^{-3}	1.1×10^{4}	0.238	3.04	[113]
TiO_2 MSM	1.9	199	6000	15000	[115]
TiO_2 MSM	1.83	889.6	13.34	11430	[116]
TiO_2 MSM	–	153	–	–	[117]
TiO_2	–	0.352	0.03	0.063	[118]
TiO_2 Schottky	–	0.897	1.12	1.46	[119]
TiO_2/SrTiO3	0.2	46.1	3.5	1400	[120]
TiO_2/NiO	0.033	181.9	717	598	[121]
TiO_2/Si	–	0.046	10	15	[122]
TiO_2/diamond	0.012	0.023	60	600	[123]
MgNiO MSM	70	1.473×10^{-4}	–	–	[134]
NiO MSM	–	4.5	266	200	[135]
NiO/IGZO	6.15×10^{-3}	0.016	–	–	[138]
NiO/ZnO	–	–	27.9	62.8	[139]
NiO/ZnO	–	0.001	0.37	0.84	[140]

References

[1] Soci C, Zhang A, Xiang B, Dayeh S A, Aplin D P R, Park J, Bao X Y, Lo Y H and Wang D 2007 *Nano Lett.* **7** 1003

[2] Aga R S, Jowhar D, Ueda A, Pan Z, Collins W E, Mu R, Singer K D and Shen J 2007 *Appl. Phys. Lett.* **91** 232108

[3] Mendoza F, Makarov V, Weiner B R and Morell G 2015 *Appl. Phys. Lett.* **107** 201605

[4] Razeghi M and Rogalski A 1996 *J. Appl. Phys.* **79** 7433

[5] Müller A, Konstantinidis G, Dragoman M, Neculoiu D, Dinescu A, Androulidaki M, Kayambaki M, Stavrinidis A, Vasilache D, Buiculescu C, Petrini I, Kostopoulos A and Dascalu D 2009 *Microelectron. J.* **40** 319

[6] Yang W F, Zhang F, Liu Z G and Wu Z Y 2008 *Mater. Sci. Semicond. Process.* **11** 59

[7] Pramanik P, Sen S, Singha C, Roy A S, Das A, Sen S and Bhattacharyya A 2016 *J. Appl. Phys.* **120** 144502

[8] Lai Y Y, Lan Y P and Lu T C 2013 *Light Sci. Appl.* **2** e76

[9] Inamdar S I and Rajpure K Y 2014 *J. Alloys Compd.* **595** 55

[10] Bai Z M, Yan X Q, Chen X, Zhao K, Lin P and Zhang Y 2014 *Prog. Nat. Sci.: Mater. Int.* **24** 1

[11] Liang F X, Zhang D Y, Wang J Z, Kong W Y, Zhang Z X, Wang Y and Luo L B 2016 *Opt. Express* **24** 25922

[12] Vikas L S, Vanaja K A, Subha P P and Jayaraj M K 2016 *Sens. Actuat. A: Phys.* **242** 116

[13] Liu K, Sakurai M and Aono M 2010 *Sensors* **10** 8604

[14] Hou Y, Mei Z and Du X 2014 *J. Phys. D: Appl. Phys.* **47** 283001

[15] Yang J L, Liu K W and Shen D Z 2017 *Chin. Phys. B* **26** 047308

[16] Zhai T Y, Fang X S, Liao M Y, Xu X J, Zeng H B, Yoshio B D and Golberg D 2009 *Sensors* **9** 6504

[17] Tian W, Lu H and Li L 2015 *Nano Res.* **8** 382

[18] Choopun S, Vispute R D, Yang W, Sharma R P, Venkatesan T and Shen H 2002 *Appl. Phys. Lett.* **80** 1529

[19] Auret F D, Goodman S A, Hayes M, Legodi M J, van Laarhoven H A and Look D C 2001 *Appl. Phys. Lett.* **79** 3074

[20] Ohtomo A, Kawasaki M, Koida T, Masubuchi K, Koinuma H, Sakurai Y, Yoshida Y, Yasuda T and Segawa Y 1998 *Appl. Phys. Lett.* **72** 2466

[21] Chen H Y, Liu K W, Hu L F, Al-Ghamdi A A and Fang X S 2015 *Mater. Today* **18** 493

[22] Yang W, Vispute R D, Choopun S, Sharma R P, Venkatesan T and Shen H 2001 *Appl. Phys. Lett.* **78** 2787

[23] Xie X, Zhang Z, Li B, Wang S, Jiang M, Shan C, Zhao D, Chen H and Shen D 2014 *Opt. Express* **22** 246

[24] Hou Y N, Mei Z X, Liang H L, Ye D Q, Gu C Z and Du X L 2013 *Appl. Phys. Lett.* **102** 153510

[25] Gold A 2010 *Appl. Phys. Lett.* **96** 242111

[26] Xie X, Zhang Z, Li B, Wang S and Shen D 2015 *Opt. Express* **23** 32329

[27] Hou Y, Mei Z, Liang H, Ye D, Gu C, Du X and Lu Y 2013 *IEEE Trans. Electron. Dev.* **60** 3474

[28] Look D C 2001 *Mater. Sci. Eng. B* **80** 383

[29] Chen H Y, Liu K W, Chen X, Zhang Z Z, Fan M M, Jiang M M, Xie X H, Zhao H F and Shen D Z 2014 *J. Mater. Chem. C* **2** 9689

[30] Özgür Ü Alivov Y I, Liu C, Teke A, Reshchikov M A, Doğan S, Avrutin V, Cho S J and Morkoç H 2005 *J. Appl. Phys.* **98** 041301

[31] Xie X H, Zhang Z Z, Shan C X, Chen H Y and Shen D Z 2012 *Appl. Phys. Lett.* **101** 081104

[32] Zheng Q H, Huang F, Ding K, Huang J, Chen D G, Zhan Z B and Lin Z 2011 *Appl. Phys. Lett.* **98** 221112

[33] Wang P, Zheng Q H, Tang Q, Yang Y T, Guo L X, Huang F, Song Z J and Zhang Z Y 2014 *Opt. Lett.* **39** 375

[34] Kind H, Yan H Q, Messer B, Law M and Yang P D 2002 *Adv. Mater.* **14** 158

[35] Chen Q, Ding H, Wu Y, Sui M, Lu W, Wang B, Su W, Cui Z and Chen L 2013 *Nanoscale* **5** 4162

[36] Zhu Y, Liu K, Wang X, Yang J, Chen X, Xie X, Li B and Shen D 2017 *J. Mater. Chem. C* **5** 7598

[37] Chen X, Liu K, Wang X, Li B, Zhang Z, Xie X and Shen D 2017 *J. Mater. Chem. C* **5** 10645

[38] Coppa B J, Davis R F and Nemanich R J 2003 *Appl. Phys. Lett.* **82** 400

[39] Azhar E A, Ye W, Helfrecht B, Chen G, Thompson L, Yu H and Dey S 2018 *IEEE Trans. Electron. Dev.* **65** 3291

[40] Liu Q, Maogang M, Cook B, Thapa P, Ewing D, Casper M, Stramel A and Wu J 2017 *Phys. Status Solidi A* **214** 1700176

[41] Coppa B J, Fulton C C, Kiesel S M, Davis R F, Pandarinath C, Burnette J E, Nemanich R J and Smith D J 2005 *J. Appl. Phys.* **97** 103517

[42] Lee S H, Kim S H and Yu J S 2016 *Nanoscale Res. Lett.* **11** 333

[43] Guo F, Yang B, Yuan Y, Xiao Z, Dong Q, Bi Y and Huang J 2012 *Nat. Nanotechnol.* **7** 798

[44] Cuong T V, Tien H N, Luan V H, Pham V H, Chung J S, Yoo D H, Hahn S H, Koo K K, Kohl P A, Hur S H and Kim E J 2011 *Phys. Status Solidi A* **208** 943

[45] Ko W, Lee S, Myoung N and Hong J 2016 *J. Mater. Chem. C* **4** 142

[46] Liu M and Kim H K 2004 *Appl. Phys. Lett.* **84** 173

[47] Angadi B, Park H C, Choi H W, Choi J W and Choi W K 2007 *J. Phys. D: Appl. Phys.* **40** 1422

[48] Reyes P I, Ku C J, Duan Z, Xu Y, Garfunkel E and Lu Y 2012 *Appl. Phys. Lett.* **101** 031118

[49] Rostami A, Dolatyari M, Amini E, Rasooli H, Baghban H and Miri S 2013 *ChemPhysChem.* **14** 554

[50] Jin Z and Wang J 2014 *J. Mater. Chem. C* **2** 1966

[51] Xu X, Shukla S, Liu Y, Yue B, Bullock J, Su L, Li Y, Javey A, Fang X and Ager J W 2018 *Phys. Status Solidi RRL* **12** 1700381

[52] Li H, Fan C, Wu G, Chen H and Wang M 2010 *J. Phys. D: Appl. Phys.* **43** 425101

[53] Sun L, Jiang D, Zhang G, Liu R, Duan Q, Qin J, Liang Q, Gao S, Hou J, Zhao J, Liu W and Shen X 2016 *J. Appl. Phys.* **119** 044508

[54] Rajan A, Kaur G, Paliwal A, Yadav H K, Gupta V and Tomar M 2014 *J. Phys. D: Appl. Phys.* **47** 425102

[55] Hwang J D, Wang F H, Kung C Y and Chan M C 2015 *IEEE Trans. Nanotechnol.* **14** 318

[56] Tian C, Jiang D, Li B, Lin J, Zhao Y, Yuan W, Zhao J, Liang Q, Gao S, Hou J and Qin J 2014 *ACS Appl. Mater. Inter.* **6** 2162

[57] Pei J, Jiang D, Zhao M, Duan Q, Liu R, Sun L, Guo Z, Hou J, Qin J, Li B and Zhang G 2016 *Appl. Surf. Sci.* **389** 1056

[58] Tong C, Yun J, Kozarsky E and Anderson W A 2013 *J. Electron. Mater.* **42** 889

[59] Li G, Song J, Zhang J and Hou X 2014 *Solid State Electron.* **92** 47

[60] Li G, Zhang J, Chen G, Ye H, Duan X and Hou X 2016 *Solid State Electron.* **123** 33

[61] Sun M W, Xu Z, Yin M, Lin Q F, Lu L F, Xue X Z, Zhu X F, Cui Y X, Fan Z Y, Ding Y L, Tian L, Wang H, Chen X Y and Li D D 2016 *Nanoscale* **8** 8924

[62] Wang X, Liu K, Chen X, Li B, Jiang M, Zhang Z, Zhao H and Shen D 2017 *ACS Appl. Mater. Inter.* **9** 5574

[63] Guo Z, Jiang D, Zhao M, Guo F, Pei J, Liu R, Sun L, Hu N and Zhang G 2016 *Solid State Electron.* **124** 24

[64] Miao J, Hu W, Jing Y, Luo W, Liao L, Pan A, Wu S, Cheng J, Chen X and Lu W 2015 *Small* **11** 2392

[65] Schoenfeld W V, Wei M, Boutwell R C and Liu H 2014 *Proc. SPIE* **8987** 89871

[66] Jiang D Y, Shan C X, Zhang J Y, Lu Y M, Yao B, Zhao D X, Zhang Z Z, Shen D Z and Yang C L 2009 *J. Phys. D: Appl. Phys.* **42** 025106

[67] Liu K W, Shen D Z, Shan C X, Zhang J Y, Jiang D Y, Zhao Y M, Yao B and Zhao D X 2008 *J. Phys. D: Appl. Phys.* **41** 125104

[68] Shukla G 2009 *IEEE Photon. Technol. Lett.* **21** 887

[69] Boutwell R C, Wei M and Schoenfeld W V 2013 *Appl. Phys. Lett.* **103** 031114

[70] Zheng Q, Huang F, Huang J, Hu Q, Chen D and Ding K 2013 *CrystEngComm* **15** 2709

[71] Fan M M, Liu K W, Zhang Z Z, Li B H, Chen X, Zhao D X, Shan C X and Shen D Z 2014 *Appl. Phys. Lett.* **105** 011117

[72] Fan M M, Liu K W, Chen X, Wang X, Zhang Z Z, Li B H and Shen D Z 2015 *ACS Appl. Mater. Inter.* **7** 20600

[73] Han S, Liu S M, Lu Y M, Cao P J, Liu W J, Zeng Y X, Jia F, Liu X K and Zhu D L 2017 *J. Alloys Compd.* **694** 168

[74] Han S, Liu S M, Liu W J, Cao P J, Lu Y M, Zeng Y X, Jia F, Liu X K, Zhu D L and Su S C 2016 *J. Phys. Chem. C* **120** 12568

[75] Han S, Ji X H, An Q L, Lu Y M, Cao P J, Liu W J, Zeng Y X, Jia F, Liu X K and Zhu D L 2017 *J. Mater. Chem. C* **5** 11472

[76] Luo W, Weng Q, Long M, Wang P, Gong F, Fang H, Luo M, Wang W, Wang Z, Zheng D, Hu W, Chen X and Lu W 2018 *Nano. Lett.* **18** 5439

[77] Zheng D, Fang H, Wang P, Luo W, Gong F, Ho J, Chen X, Lu W, Liao L, Jianlu Wang J and Hu W 2016 *Adv. Funct. Mater.* **26** 7690

[78] Zheng D, Wang J, Hu W, Liao L, Fang H, Guo N, Wang P, Gong F, Wang X, Fan Z, Wu X, Meng X, Chen X and Lu W 2016 *Nano Lett.* **16** 2548

[79] Chen Y, Wang X, Wang P, Huang H, Wu G, Tian B, Hong Z, Wang Y, Sun S, Shen H, Wang J, Hu W, Sun J, Meng X and Chu J 2016 *ACS Appl. Mater. Inter.* **8** 32083

[80] Wang X, Wang P, Wang J, Hu W, Zhou X, Guo N, Huang H, Sun S, Shen H, Lin T, Tang M, Liao L, Jiang A, Sun J, Meng X, Chen X, Lu W and Chu J 2015 *Adv. Mater.* **27** 6575

[81] Wang J L, Fang H H, Wang X D, Chen X S, Lu W and Hu W D 2017 *Small* **13** 1700894

[82] Tian H, Wang X, Zhu Y, Liao L, Wang X, Wang J and Hu W 2017 *Appl. Phys. Lett.* **110** 043505

[83] Wang P, Wang Y, Ye L, Wu M, Xie R, Wang X, Chen X, Fan Z, Wang J and Hu W 2018 *Small* **14** 1800492

[84] Wang Y, Wang P, Zhu Y, Gao J, Gong F, Li Q, Xie R, Wu F, Wang D, Yang J, Fan Z, Wang X and Hu W 2019 *Appl. Phys. Lett.* **114** 011103

[85] Wang J and Hu W 2017 *Chin. Phys. B* **26** 037106

[86] Xu M, Ge L, Han M, Huang J, Xu H and Yang Z 2019 *Chin. Phys. B* **28** 028502

[87] Suzuki R, Nakagomi S and Kokubun Y 2011 *Appl. Phys. Lett.* **98** 131114

[88] Ji Z G, Du J, Fan J and Wang W 2006 *Opt. Mater.* **28** 415

[89] Rafique S, Han L and Zhao H P 2017 *Phys. Status Solidi A* **214** 1700063

[90] Ghose S, Rahman S, Hong L, Rojas-Ramirez J S, Jin H, Park K, Klie R and Droopad R 2017 *J. Appl. Phys.* **122** 095302

[91] Orita M, Ohta H, Hirano M and Hosono H 2000 *Appl. Phys. Lett.* **77** 4166

[92] Oshima T, Okuno T and Fujita S 2007 *Jpn. J. Appl. Phys.* **46** 7217

[93] Weng W Y, Hsueh T J, Chang S J, Huang G J and Hsueh H T 2011 *IEEE Sens. J.* **11** 999

[94] Wei T C, Tsai D S, Ravadgar P, Ke J J, Tsai M L, Lien D H, Huang C Y, Horng R H and He J H 2014 *IEEE J. Sel. Top. Quantum Electron.* **20** 3802006

[95] Yu F P, Ou S L and Wuu D S 2015 *Opt. Mater. Express* **5** 1240

[96] Wu Z H, Qian L X, Sheng T, Zhang Y Y and Liu X Z 2016 *IEEE Int. Conf. Electron. Devices Solid-State Circuits* 82

[97] Liu X Z, Guo P, Sheng T, Qian L X, Zhang W L and Li Y R 2016 *Opt. Mater.* **51** 203

[98] Cui S J, Mei Z X, Zhang Y H, Liang H L and Du X L 2017 *Adv. Opt. Mater.* **5** 1700454

[99] Qian Y P, Guo D Y, Chu X L, Shi H Z, Zhu W K, Wang K, Huang X K, Wang H, Wang S L, Li P G, Zhang X H and Tang W H 2017 *Mater. Lett.* **209** 558

[100] Li P G, Shi H Z, Chen K, Guo D Y, Cui W, Zhi Y S, Wang S L, Wu Z P, Chen Z W and Tang W H 2017 *J. Mater. Chem. C* **5** 10562

[101] Wu Z P, Jiao L, Wang X L, Guo D Y, Li W H, Li L H, Huang F and Tang W H 2017 *J. Mater. Chem. C* **5** 8688

[102] An Y H, Zhi Y S, Wu Z P, Cui W, Zhao X L, Guo D Y, Li P G and Tang W H 2016 *Appl. Phys. A* **122** 1036

[103] Nakagomi S, Momo T, Takahashi S and Kokubun Y 2013 *Appl. Phys. Lett.* **103** 072105

[104] Kokubun Y, Miura K, Endo F and Nakagomi S 2007 *Appl. Phys. Lett.* **90** 031912

[105] Guo D Y, Wu Z P, An Y H, Guo X C, Chu X L, Sun C L, Li L H, Li P G and Tang W H 2014 *Appl. Phys. Lett.* **105** 023507

[106] Hu G C, Shan C X, Zhang N, Jiang M M, Wang S P and Shen D Z 2015 *Opt. Express* **23** 13554

[107] Alema F, Hertog B, Ledyaev O, Volovik D, Thoma G, Miller R, Osinsky A, Mukhopadhyay P, Bakhshi S, Ali H and Schoenfeld W V 2017 *Phys. Status Solidi A* **214** 1600688

[108] Zhang D, Zheng W, Lin R C, Li T T, Zhang Z J and Huang F 2018 *J. Alloys Compd.* **735** 150

[109] Chen X, Liu K W, Zhang Z Z, Wang C R, Li B H, Zhao H F, Zhao D X and Shen D Z 2016 *ACS Appl. Mater. Inter.* **8** 4185

[110] Weng W Y, Hsueh T J, Chang S J, Huang G J and Hsueh H T 2011 *IEEE. Sens. J.* **11** 1491

[111] Guo X C, Hao N H, Guo D Y, Wu Z P, An Y H, Chu X L, Li L H, Li P G, Lei M and Tang W H 2016 *J. Alloys Compd.* **660** 136

[112] Qu Y Y, Wu Z P, Ai M L, Guo D Y, An Y H, Yang H J, Li L H and Tang W H 2016 *J. Alloys Compd.* **680** 247
[113] Chen X H, Xu Y, Zhou D, Yang S, Ren F F, Lu H, Tang K, Gu S L, Zhang R, Zheng Y D and Ye J D 2017 *ACS Appl. Mater. Inter.* **9** 36997
[114] Zou J, Zhang Q, Huang K and Marzari N 2010 *J. Phys. Chem. C* **114** 10725
[115] Xue H L, Kong X Z, Liu Z R, Liu C X, Zhou J R and Chen W Y 2007 *Appl. Phys. Lett.* **90** 201118
[116] Kong X Z, Liu C X, Dong W, Zhang X D, Tao C, Shen L, Zhou J R, Fei Y F and Ruan S P 2009 *Appl. Phys. Lett.* **94** 123502
[117] Shih W S, Young S J, Ji L W, Water W, Meen T H and Shiu 2011 *IEEE Sens. J.* **11** 3031
[118] Akbari M K, Hai Z Y, Depuydt S, Kats E, Hu J and Zhuiykov S 2017 *IEEE. Trans. Nanotechnol.* **16** 880
[119] Patel D B, Chauhan K R, Park W H, Kim H S, Kim J and Yun J H 2017 *Mat. Sci. Semicon. Proc.* **61** 45
[120] Zhang M, Zhang H F, Lv K B, Chen W Y, Zhou J R, Shen L and Ruan S P 2012 *Opt. Express* **20** 5936
[121] Zhang D Z, Liu C Y, Xu R L, Yin B, Chen Y, Zhang X D, Gao F L and Ruan S P 2017 *Nanotechnology* **28** 365505
[122] Sun L, Wang C R, Ji T, Wang J L, Yi G C and Chen X S 2017 *RSC Adv.* **7** 51744
[123] Liu Z C, Ao J P, Li F N, Wang W, Wang J J, Zhang J W and Wang H X 2017 *Mater. Lett.* **188** 52
[124] Hakim A, Hossain J and Khan K 2009 *Renew. Energ.* **34** 2625
[125] Al-Ghamdi A A, Abdel-wahab M S, Farghali A A and Hasan P M Z 2016 *Mater. Res. Bull.* **75** 71
[126] Ahmed A A, Afzal N, Devarajan M and Subramani S 2016 *Mater. Res. Express* **3** 116405
[127] Caruge J M, Halpert J E, Wood V, Bulovic V and Bawendi M G 2008 *Nat. Photon.* **2** 247
[128] Waser R and Aono M 2007 *Nat. Mater.* **6** 833
[129] Gibson E A, Smeigh A L, Pleux L L, Fortage J, Boschloo G, Blart E, Pellegrin Y, Odobel F, Hagfeldt A and Hammarstrom L 2009 *Angew. Chem. Int. Ed.* **121** 4466
[130] Mallows J, Planells M, Thakare V, Bhosale R, Ogale S and Robertson N 2015 *ACS Appl. Mater. Inter.* **7** 27597
[131] Park N, Sun K, Sun Z L, Jing Y and Wang D L 2013 *J. Mater. Chem. C.* **1** 7333
[132] Kim D Y, Ryu J, Manders J, Lee J and So F 2014 *ACS Appl. Mater. Inter.* **6** 1370
[133] Kim H, Kumar M D, Patel M and Kim J 2016 *Mater. Res. Bull.* **83** 35
[134] Zhao Y M, Zhang J Y, Jiang D Y, Shan C X, Zhang Z Z, Yao B, Zhao D X and Shen D Z 2009 *J. Phys. D: Appl. Phys.* **42** 092007
[135] Ahmed A A, Devarajan M and Afzal N 2017 *Sens. Actuat. A: Phys.* **262** 78
[136] Choi J M and Im S 2005 *Appl. Surf. Sci.* **244** 435
[137] Zhang D Y, Nozaki S J and Uchida K 2014 *J. Vac. Sci. Technol. B* **32** 031202
[138] Li H K, Chen T P, Hu S G, Li X D, Liu Y, Lee P S, Wang X P, Li H Y and Lo G Q 2015 *Opt. Express* **23** 27683
[139] Tsai S Y, Hon M H and Lu Y M 2011 *Mater. Sci. Forum* **687** 711
[140] Patel M and Kim J 2017 *J. Alloys Compd.* **729** 796